Human Molecular Genetics, 2006, Vol. 15, No. 1 **33–44**
doi:10.1093/hmg/ddi423
Advance Access published on November 25, 2005

Proteasome impairment does not contribute to pathogenesis in R6/2 Huntington's disease mice: exclusion of proteasome activator REGγ as a therapeutic target

John S. Bett[1], Geoffrey M. Goellner[2], Ben Woodman[1], Gregory Pratt[2], Martin Rechsteiner[2] and Gillian P. Bates[1,*]

[1]Department of Medical and Molecular Genetics, GKT School of Medicine, King's College London, 8th Floor Guy's Tower, Guy's Hospital, London SE1 9RT, UK and [2]Department of Biochemistry, University of Utah School of Medicine, 50 N Medical Drive, Salt Lake City, UT 84132, USA

Received September 22, 2005; Accepted November 10, 2005

Huntington's disease (HD) is one of a group of neurodegenerative disorders caused by the pathological expansion of a glutamine tract. A hallmark of these so-called polyglutamine diseases is the presence of ubiquitylated inclusion bodies, which sequester various components of the 19S and 20S proteasomes. In addition, the ubiquitin–proteasome system (UPS) has been shown to be severely impaired *in vitro* in cells overexpressing mutant huntingtin. Thus, because of its fundamental housekeeping function, impairment of the UPS in neurons could contribute to neurotoxicity. We have recently proposed that the proteasome activator REGγ could contribute to UPS impairment in polyglutamine diseases by suppressing the proteasomal catalytic sites responsible for cleaving Gln–Gln bonds. Capping of proteasomes with REGγ could therefore contribute to a potential 'clogging' of the proteasome by pathogenic polyglutamines. We show here that genetic reduction of REGγ has no effect on the well-defined neurological phenotype of R6/2 HD mice and does not affect inclusion body formation in the R6/2 brain. Surprisingly, we observe increased proteasomal 'chymotrypsin-like' activity in 13-week-old R6/2 brains relative to non-R6/2, irrespective of REGγ levels. However, assays of 26S proteasome activity in mouse brain extracts reveal no difference in proteolytic activity regardless of R6/2 or REGγ genotype. These findings suggest that REGγ is not a viable therapeutic target in polyglutamine disease and that overall proteasome function is not impaired by trapped mutant polyglutamine in R6/2 mice.

INTRODUCTION

Huntington's disease (HD) belongs to a devastating group of neurodegenerative diseases caused by the pathogenic expansion of a CAG trinucleotide within the disease gene. These polyglutamine diseases include spinal and bulbar muscular atrophy (SBMA), dentatorubral pallidoluysian atrophy and spinocerebellar ataxia types 1, 2, 3, 6, 7 and 17. For most of the polyglutamine diseases, there exists a sharp threshold for disease. In HD, individuals with repeats of 35 or less will remain unaffected, whereas in those patients with 40 or more repeats, the disease will manifest in a normal lifetime.

A common pathogenic marker in HD and other polyglutamine diseases is the presence of proteinaceous aggregates which can culminate as an inclusion body inside or outside of neuronal nuclei. These inclusions are present in HD mouse (1) and human brains (2), although their pathological significance is widely debated. Evidence that the aggregation process is dependent on a pathogenic polyglutamine length is incontrovertible (3), and directing pre-formed polyglutamine

*To whom correspondence should be addressed. Tel: +44 2071883722; Fax: +44 2071882585; Email: gillian.bates@genetics.kcl.ac.uk

inclusions to the nucleus is toxic to the cell (4). However, the possibility that inclusion body formation is controlled in the neuron as a cytoprotective response could mean that the mere presence of an inclusion body is not necessarily as pathogenic as the presence of soluble mutant polyglutamine or smaller oligomeric aggregates (5–7).

The ubiquitin–proteasome system (UPS) is an essential part of cellular housekeeping, which degrades proteins that are tagged with four or more ubiquitin monomers. The fact that inclusion bodies are polyubiquitylated suggests that the UPS has made futile attempts to degrade components of the inclusion. Indeed, once polyglutamine proteins have aggregated in an inclusion, they are resistant to degradation by the UPS (8). The UPS is further implicated in polyglutamine pathogenesis by the fact that various components of the 26S proteasome are sequestered to inclusions, suggesting that the UPS may be actively engaged in an attempt to degrade components of the inclusions (9,10). Direct evidence of UPS dysfunction in polyglutamine disease came from a cell model overexpressing mutant huntingtin, where a dramatic accumulation of a GFP-based UPS reporter containing the CL-1 degron was observed (11,12). Although this effect has also been observed in an ataxin-1 cell model (13), no impairment was observed in an HD cell model expressing a UPS reporter with an N-end rule or a ubiquitin fusion degradation (UFD) signal (8).

It is currently unknown how the UPS is involved in the pathogenesis of polyglutamine disease *in vivo*. Recent evidence from an SCA7 mouse model shows that polyglutamine pathogenesis can occur in photoreceptor cells in the absence of any significant UPS impairment, as detected by a UFD-based reporter (14). In addition, no impairment in core proteasome activity was found in *Hdh*CAG150 knock-in mouse brains (15), whereas HD94 conditional mice show an upregulation in this activity (16). However, in human HD brain and fibroblasts, a diminution in core proteasome activity has been described, evidence of a proteasome disturbance in symptomatic patients (17).

There is strong evidence that proteins with a mutant polyglutamine tract are intrinsically difficult to degrade (18,19). Indeed, more recent data suggest that polyglutamine tracts are not degraded at all by eukaryotic proteasomes (20). However, it has also been shown that cells expressing mutant polyglutamines directed to the UPS show reduced inclusion formation (21,22). This suggests that although polyglutamine tracts are intrinsically difficult to degrade, directing them to the UPS is still overall sufficient to increase their degradation.

We have recently hypothesized that the nuclear proteasome activator REGγ may be contributing to polyglutamine pathogenesis, largely due to our *in vitro* data which suggest that it can inhibit proteasomal cleavage between Gln–Gln bonds and the fact that it is enriched in the brain (23,24). REGγ binds to the 20S proteasome as a doughnut-shaped homoheptamer and alters the cleavage specificity of the three-core proteasome active sites. We have shown that REGγ activates the trypsin-like active site *in vitro*, but suppresses the chymotrypsin-like and peptidyl–glutamyl preferring hydrolytic (PGPH) active sites, which are responsible for cleaving Gln–Gln bonds (23). Furthermore, a REGγ mutant (K118E) is capable of activating all three catalytic activities and promoting cleavage after glutamines (24). Thus, we have proposed that mutant polyglutamines may become kinetically trapped in proteasomes capped with REGγ causing 'clogging' of proteasomes and contributing to neurotoxicity. We have tested this hypothesis *in vivo* by crossing REGγ-deficient mice to R6/2 HD mice. REGγ KO mice have been generated previously and are viable, but slightly growth impaired (25). We found that the genetic reduction of REGγ did not alleviate the neurological phenotype of R6/2 mice and did not alter inclusion body formation in the R6/2 brain. In addition, we report that 'chymotrypsin-like' proteasome activity is upregulated in the R6/2 brain regardless of REGγ levels, whereas there is no change in 26S proteasome activity. Our results suggest that REGγ is not involved in polyglutamine disease and that there is no net proteasome impairment in the R6/2 mouse brain as a result of trapped mutant polyglutamine.

RESULTS

REGγ protein levels are unchanged in R6/2 brains and absent in nulls

A common feature of polyglutamine disease is transcriptional dysregulation, resulting in altered levels of affected proteins. Indeed, neurons may even attempt to upregulate or downregulate certain genes as a response to disease progression. Therefore, before determining the effect of reducing REGγ protein levels on the well-defined neurological phenotype of R6/2, it was important to establish that basic REGγ levels were unaltered in the R6/2 brain as a result of the disease process. Western blot analysis and subsequent phosphorimager quantification revealed that REGγ levels were similar in brain lysates of 12-week-old R6/2 compared to that of wild-type (WT) (Fig. 1A). Next, to ensure that protein levels of REGγ were reduced as expected in heterozygous and null mice, western blot analysis was applied to brain lysates. Levels of REGγ were found to be approximately halved in heterozygotes and completely absent in null mice as expected (Fig. 1B). We also sought to determine whether the genetic reduction of REGγ would cause an alteration in the protein expression of REGα, a homologue of REGγ. We found that REGα levels were unaltered by the reduction of REGγ (Fig. 1B). This is in good agreement with Murata *et al.* (25), who found that REGα expression was unchanged in REGγ-deficient mouse embryonic fibroblasts. In addition, they reported no change in the cytoplasmic localization of REGα, suggesting that it does not enter the nucleus to compensate for the REGγ deficiency.

REGγ is located in neuronal nuclei in both WT and R6/2 mice

Central to the hypothesis that REGγ-capped proteasomes contribute to polyglutamine pathogenesis is the localization of REGγ to the nucleus, a major site of inclusion body formation and pathogenesis in polyglutamine disease. Previous work has demonstrated a predominant nuclear localization of REGγ in neuronal cell lines (26), *Drosophila* embryos (27) and cultured mouse embryonic fibroblasts (25). To confirm localization of

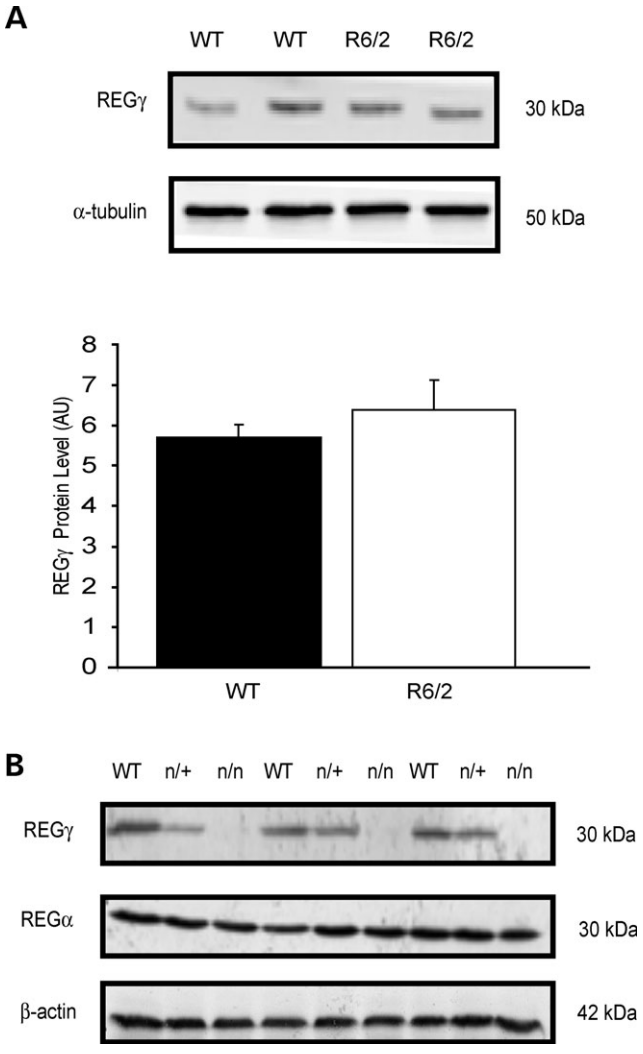

Figure 1. Protein levels of REGγ and REGα in mouse brain. (**A**) REGγ levels are unaltered in 12-week R6/2 brains, as shown by western blot and phosphoimager quantification with respect to α-tubulin. Error bars show the standard error of the mean (Student's *t*-test, $P = 0.419$). (**B**) REGγ levels are halved in heterozygous mice and absent in null mice as expected. REGα levels are unaltered by the loss of REGγ. β-actin was used as a loading control. n, null allele.

REGγ in the mouse brain, immunohistochemistry was performed on coronal sections. REGγ was found to be highly expressed and has a nuclear localization throughout the mouse brain. A representative image from mouse cortex is shown in Figure 2A. The lack of any specific staining in REGγ null mice confirms that the protein is absent in these mice and that the antibody is specific (Fig. 2A). To confirm the subcellular localization of REGγ biochemically, western blot analysis was performed on 12-week-old nuclear and cytoplasmic brain fractions. It is clear that REGγ is present only in the nuclear fraction and that its subcellular location is unaltered in the R6/2 brain (Fig. 2B). Finally, to distinguish between the possibility that REGγ is expressed in neurons or glia, colocalization studies were carried out between the REGγ and the neuronal marker NeuN. We found that REGγ is expressed mainly in neurons and little, if any, was detected outside of neurons. A representative image from WT mouse cortex can be seen in Figure 2C.

Reduction of REGγ does not affect the behavioural phenotype of R6/2 mice

Once we had confirmed that REGγ is located in mouse neuronal nuclei and that protein levels are efficiently reduced in heterozygous and null mice, it was possible to cross REGγ-deficient mice to R6/2 and investigate the effect of REGγ reduction on R6/2 neurological behaviour. Five-week-old R6/2 males were crossed to heterozygous REGγ females to generate males of the genotype R6/2; REGγ$^{n/+}$ (n = null allele). These males were then backcrossed to REGγ$^{n/+}$ females to generate six possible genotypes: REGγ$^{+/+}$, REGγ$^{n/+}$ or REGγ$^{n/n}$ on an R6/2 or non-R6/2 background. The CAG repeat size of the R6/2 mice was well matched. CAG repeat means were as follows: R6/2 = 222.5; R6/2; REGγ$^{n/+}$ = 224.3; R6 and REGγ$^{n/n}$ = 223.5. Ten to 15 females of each genotype were divided equally between cages to ensure a variety of genotypes from different litters were present in each cage. The mice were tested for rotarod performance, grip strength and exploratory activity, and their weight was monitored weekly.

Rotarod is a sensitive test of motor coordination and balance, and R6/2 mice have been previously shown to have impaired rotarod performance from ~6 weeks (28,29). We found that R6/2 mice performed significantly worse on rotarod than non-R6/2 mice at all timepoints tested (Fig. 3A). For example, at 12 weeks, R6/2 performed significantly worse than non-R6/2 [General Linear Model (GLM) ANOVA: $F_{(1,59)} = 50.2$, $P < 0.001$]. The genetic reduction of REGγ did not affect the impairment in R6/2 performance at any timepoint, e.g. there was no interaction between R6/2 and REGγ genotypes at 12 weeks (GLM ANOVA: $F_{(2,58)} = 0.97$, $P = 0.386$). Interestingly, REGγ$^{n/n}$ mice performed significantly worse than REGγ$^{+/+}$ or REGγ$^{n/+}$ at 4 weeks (*post hoc* analysis: $T = 2.812$, $P = 0.0181$ and $T = 3.737$, $P = 0.0012$, respectively), whether or not they expressed the R6/2 transgene [no interaction between REGγ and R6/2 genotypes (GLM ANOVA: $F_{(2,58)} = 0.12$, $P = 0.889$)]. REGγ$^{n/n}$ mice were also significantly worse than REGγ$^{+/+}$ at 8 weeks (*post hoc* analysis: $T = 3.055$, $P = 0.0093$), but not significantly different from REGγ$^{n/+}$ (*post hoc* analysis: $T = 2.158$, $P = 0.0871$). By 10 weeks, there was no significant difference between the REGγ genotypes (GLM ANOVA: $F_{(2,58)} = 0.22$, $P = 0.803$) or at 12 weeks (GLM ANOVA: $F_{(2,58)} = 0.22$, $P = 0.802$), suggesting that the rotarod impairment in REGγ nulls is present only at a young age and could possibly be attributed to retarded growth (Fig. 3D).

Grip strength analysis showed that R6/2 mice had a significantly weaker grip than non-R6/2 by 12 weeks (GLM ANOVA: $F_{(1,59)} = 49.57$, $P < 0.001$) (Fig. 3B) and this was regardless of REGγ genotype [no interaction between R6/2 and REGγ genotypes at 12 weeks (GLM ANOVA: $F_{(2,58)} = 0.33$, $P = 0.717$)]. In addition, although R6/2 mice gain significantly less weight than non-R6/2 mice (12 weeks GLM ANOVA: $F_{(1,59)} = 4.59$, $P = 0.036$) (Fig. 3C), REGγ genotype has no effect on this failure to gain weight

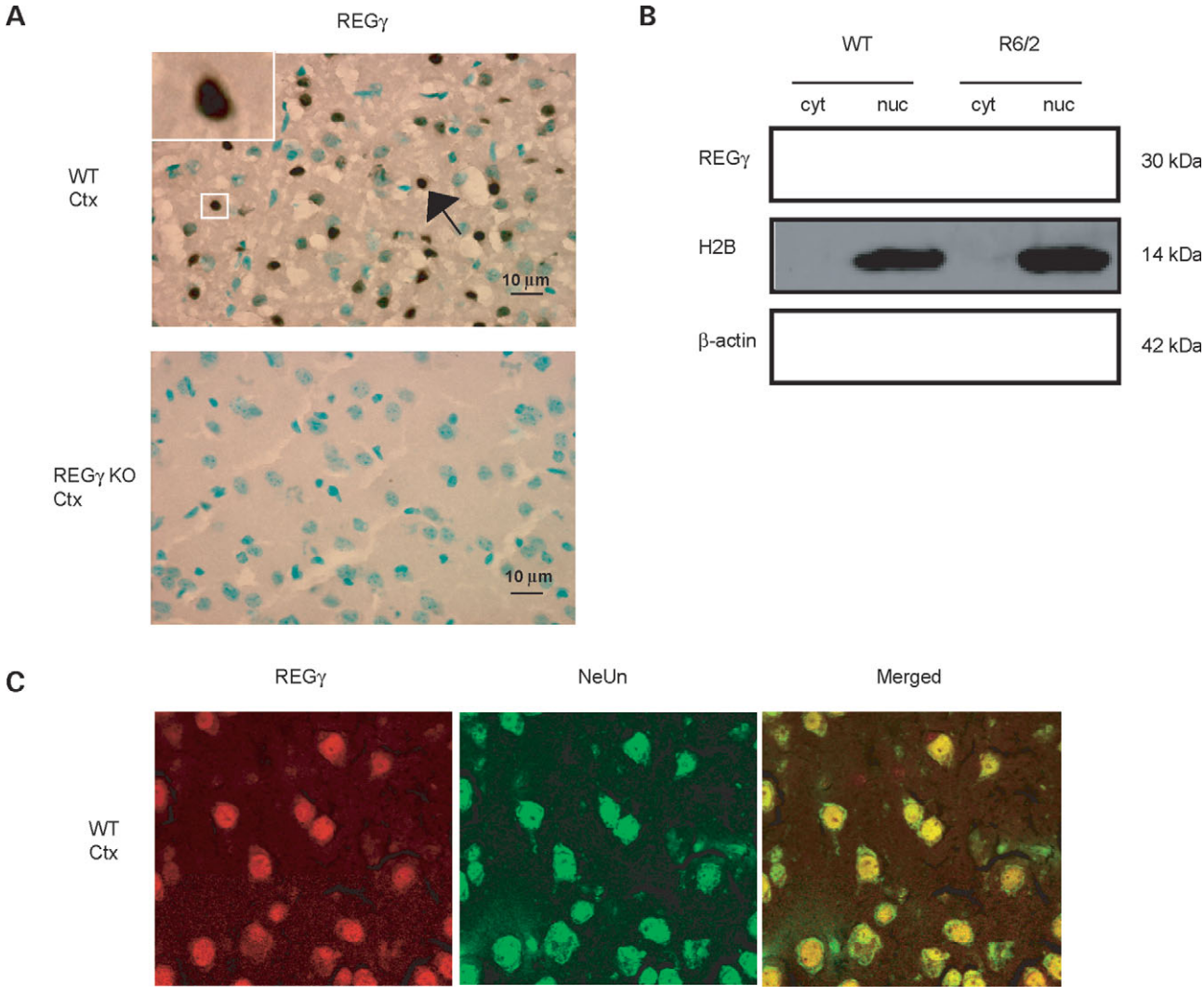

Figure 2. REGγ is highly expressed in the mouse brain and is restricted to neuronal nuclei. (**A**) Coronal sections through cortex of WT and REGγ null mouse brain reveal a predominant nuclear localization of REGγ. The absence of any specific staining in the null mice confirms that REGγ has been successfully knocked out and that the antibody is specific. Arrow points to a nucleus expressing REGγ, and inset shows higher magnification of another nucleus expressing REGγ. The nuclear counterstain is methyl green. (**B**) Western blot analysis on nuclear and cytoplasmic 12-week-old brain fractions confirms that REGγ has a nuclear localization. Blots were stained with histone H2B as a nuclear marker and β-actin as a cytoplasmic marker. (**C**) REGγ colocalizes with the neuronal marker NeuN in the mouse brain. No REGγ was detected in glial cells. Ctx, cortex; cyt, cytoplasm and nuc, nucleus.

(no interaction at 12 weeks, GLM ANOVA: $F_{(2,58)} = 0.09$, $P = 0.918$). We also observed that REGγ$^{n/n}$ mice weighed significantly less than heterozygous or WT mice until 8 weeks (e.g. GLM ANOVA: $F_{(2,58)} = 3.55$, $P = 0.035$ for 8 weeks), but this effect was gone by 9 weeks (GLM ANOVA: $F_{(2,58)} = 2.93$, $P = 0.061$) (Fig. 3D). This is consistent with the growth deficits of REGγ null mice observed previously (25), and interestingly, the effect is lost at approximately the same age as the disappearance of rotarod impairment in REGγ null mice, supporting a role for REGγ in post-natal mouse development.

Exploratory activity revealed an overall hypoactivity of R6/2 mice compared with non-R6/2 mice at 13 weeks, where *P*-values were less than 0.004 for all parameters tested (Fig. 4). For most parameters tested, REGγ had no effect on R6/2 hypoactivity, although there was a significant negative interaction between R6/2 and REGγ genotypes for activity and rearing (GLM ANOVA: $F_{(2,58)} = 3.31$, $P = 0.043$ and $F_{(2,58)} = 3.79$, $P = 0.029$, respectively). REGγ did not affect R6/2 activity at 6 or 9 weeks (data not shown).

Inclusion formation in the R6/2 brain is not modified by reduction of REGγ

Although reduction of REGγ levels did not alter the behavioural phenotype of R6/2, it remained a possibility that its genetic reduction altered inclusion formation as a result of differential processing of the R6/2 transprotein by REGγ-capped proteasomes. A similar effect has previously been observed whereby early inclusion formation in R6/2 can be modified by overexpression of Hsp70 without affecting the

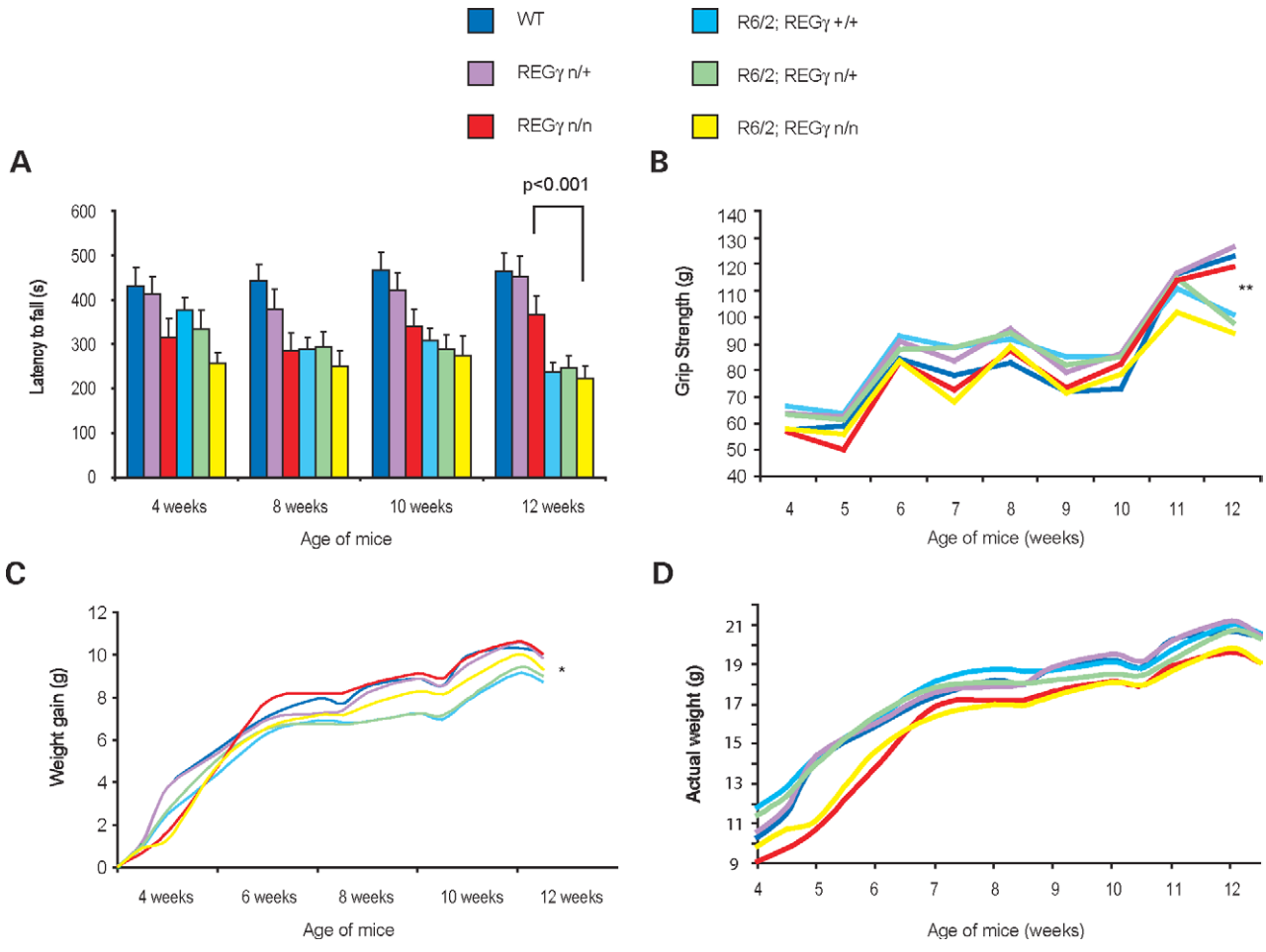

Figure 3. Genetic reduction of REGγ does not affect R6/2 rotarod performance, grip strength or failure to gain weight. Animal numbers were as follows. WT: $n = 10$, R6/2; REGγ$^{+/+}$: $n = 13$, REGγ$^{n/+}$: $n = 12$, R6/2; REGγ$^{n/+}$: $n = 12$, REGγ$^{n/n}$: $n = 10$, R6/2 and REGγ$^{n/n}$: $n = 10$. Error bars represent standard errors of the mean. (**A**) Rotarod performance of R6/2 mice is significantly lower than that of non-R6/2 from 4 weeks onwards and REGγ has no effect on R6/2 performance. REGγ$^{n/n}$ mice perform significantly worse than REGγ$^{n/+}$ or REGγ$^{+/+}$ at 4 and 8 weeks, but not at 10 or 12 weeks. (**B**) Graph showing grip strength performance of mice. R6/2 mice perform significantly worse than non-R6/2 at 12 weeks regardless of REGγ levels. (**C**) Weight gain of R6/2 mice is significantly lower than that of non-R6/2 mice. (**D**) Actual weight of mice shows that REGγ$^{n/n}$ mice weigh significantly less than others until ~9 weeks of age. Dips in weight and weight gain observed at 8, 10 and 12 weeks can be attributed to weight loss as a result of rotarod exercise. $^{*}P = 0.036$; $^{**}P < 0.001$.

behavioural phenotype (30). To address this issue, we adopted a qualitative immunohistochemical approach, where we compared inclusion formation in the CA1 region of the hippocampus. We chose this region as REGγ is expressed there, and it provides a precise location that allows a fair comparison of inclusion formation between brains. From three brains of all three genotypes, seven sections of each were stained in parallel with S830 anti-huntingtin antibody, which can be used to monitor inclusion formation in the R6/2 hippocampus (31). We used 4-week-old brain sections because at this age, inclusion formation is still at an early stage, allowing any potential difference between REGγ genotypes to be more easily detected. Comparison of inclusion formation in R6/2 with reduced or knocked out REGγ revealed no obvious difference in overall size or amount of inclusions (Fig. 5). We also compared inclusion formation qualitatively at 13 weeks and found no obvious differences caused by REGγ reduction (data not shown). This suggests that the association of REGγ with proteasomes does not affect the processing of mutant polyglutamine and/or inclusion body formation in R6/2 mice.

Core 20S proteasome activity is upregulated in R6/2 brains

We next investigated core proteasome activity in whole brain extracts of R6/2 and WT mice. This would highlight any alteration of the UPS in the R6/2 brain at the level of the 20S proteasome or its association with activators. We measured the degradation of the fluorogenic peptide sLLVY-MCA as a reliable reporter of proteasomal chymotrypsin-like activity, but did not find substrates that were completely specific for the trypsin-like or PGPH-like activities (data not shown). We found that there was no difference in chymotrypsin-like proteasome activity between R6/2 and WT at 4 or 8 weeks regardless of REGγ levels [e.g. no

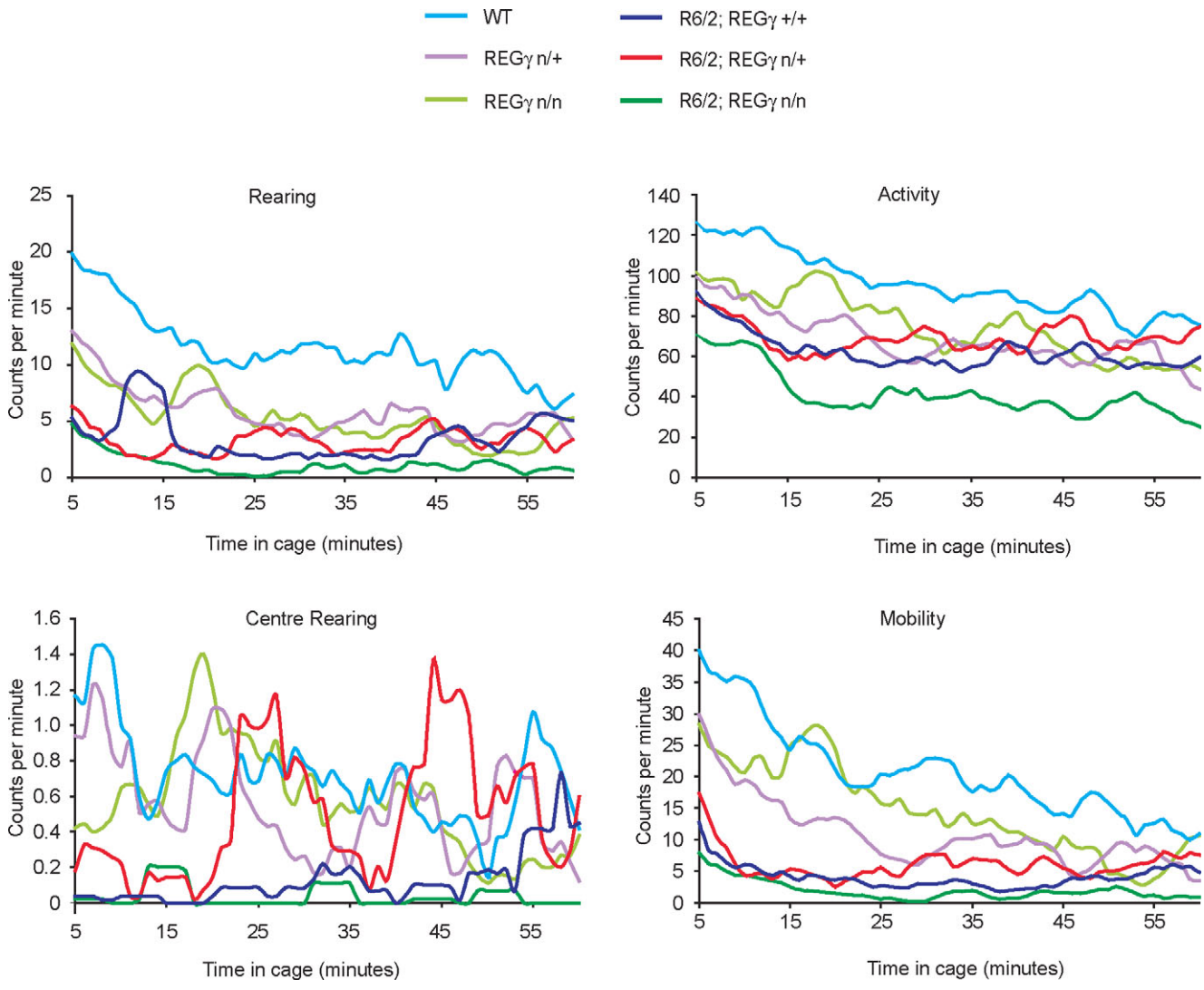

Figure 4. Exploratory activity of 13-week-old mice displayed as 5 min moving averages. Activity cage data reveal an overall hypoactivity of R6/2 mice compared to non-R6/2 for rearing ($P < 0.001$), activity ($P = 0.002$), centre rearing ($P = 0.004$) and mobility ($P < 0.001$). The reduction of REGγ did not improve the hypoactivity of R6/2.

interaction between REGγ and R6/2 genotypes at 4 weeks (GLM ANOVA: $F_{(1,39)} = 0.72$, $P = 0.491$)] (Fig. 6A). Although the graph suggests that REGγ depletion causes a reduction in chymotrypsin-like activity, this falls just out of significance (GLM ANOVA: $F_{(1,39)} = 2.76$, $P = 0.076$). Surprisingly, by 13 weeks, chymotrypsin-like activity was significantly upregulated in R6/2 than in non-R6/2 (GLM ANOVA: $F_{(1,48)} = 17.04$, $P < 0.001$) (Fig. 6A), irrespective of REGγ levels.

Levels of various proteasomal proteins are unaltered in R6/2 brains

To investigate the potential reasons for the upregulation of 20S core activity in R6/2, we compared protein levels of various proteasome or proteasome-associated subunits between 12-week R6/2 and WT brains. We first looked for a direct upregulation of 20S proteasome (32), but found no significant upregulation in R6/2 corresponding to the increase in 20S activity (Fig. 6B). We also failed to find a difference in levels of the 19S S10B subunit (33) in 12-week-old R6/2 brains (Fig. 6B). It has previously been reported that an upregulation of proteasome activity in HD94 mice was linked to an increase in the inducible immunoproteasome subunits LMP2 and LMP7 (16). However, the levels of these proteins were not significantly different between R6/2 and WT mice at 12 weeks (Fig. 6B). Finally, because the association of proteasomes with the 11S activators can markedly stimulate 20S activity, we compared levels of the activator REGα between R6/2 and WT brains, but found no significant difference (Fig. 6B). Nor was there a difference in REGγ levels (Fig. 1). Therefore, we detected no upregulation of proteasomal proteins, which may account for the increase in 20S activities in R6/2.

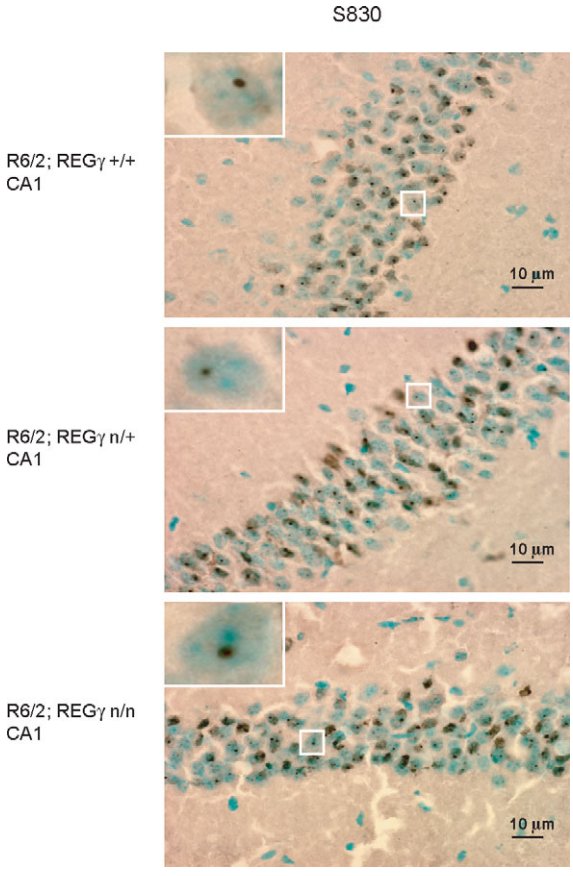

Figure 5. Comparison of inclusion body formation in 4-week R6/2 mouse brains that are REGγ$^{+/+}$, REGγ$^{n/+}$ or REGγ$^{n/n}$. The CA1 region of the hippocampus was used for comparison. No obvious difference was apparent in the different genotypes. Insets show higher magnification of inclusion bodies.

26S proteasome activity is unchanged in R6/2

Although we observed an upregulation of 20S activity in R6/2 than in WT, this did not exclude the possibility that there was an impairment in 26S proteasome activity in the R6/2 brain. To compare 26S proteasome activity between R6/2 and WT, we measured the *in vitro* degradation of radiolabelled ubiquitylated lysozyme by mouse whole brain extracts. This assay would detect any impairment of R6/2 brain extracts in the recognition of a ubiquitylated substrate, its unfolding by the 19S proteasome and subsequent degradation by the 20S core. We found that there was no difference in 26S proteasome activity between R6/2 and non-R6/2 at any timepoint (e.g. 13-week GLM ANOVA: $F_{(1,48)} = 1.51$, $P = 0.225$) and REGγ genotype had no effect (Fig. 7). Therefore, we detected no impairment of the 26S proteasome in the R6/2 brain.

DISCUSSION

We have recently hypothesized that the nuclear proteasome activator REGγ may contribute to pathogenesis in polyglutamine disease by preventing proteasomes from cleaving within polyglutamine stretches (24). REGγ is homologous to the cytoplasmic proteasome activators, REGα and REGβ, which are involved in the generation of peptides for antigen presentation. Proteasome activators can markedly increase the *in vitro* degradation of small peptides specific for some or all of the three proteasomal catalytic sites, possibly by controlling the opening of proteasomal entry and exit gates (reviewed in 34). It is unknown exactly how *in vitro* activation properties are biologically relevant, but one possibility is that proteasome activators bind to 26S proteasomes and thus alter the proteasomal cleavage sites within ubiquitylated proteins.

Although REGα and REGβ stimulate all three proteasome catalytic sites *in vitro*, REGγ has been shown to stimulate only the trypsin-like site, but suppresses the activation of the chymotrypsin-like and PGPH active sites (23). These are the sites responsible for hydrolysing Gln–Gln bonds. In addition, it is highly expressed in the brain and localized to the nucleus, a major site of polyglutamine pathology. We hypothesized that mutant proteins with a polyglutamine tract of over 40 repeats may therefore become kinetically trapped inside proteasome chambers capped with REGγ, which would be consistent with the finding that peptides greater than 40 residues are rarely found in proteasomal digests.

In this study, we have rigorously tested this hypothesis. We found that reducing or knocking out REGγ protein levels did not improve the behaviour of R6/2 mice, did not alter the inclusion formation in the R6/2 brain and failed to affect proteasome activities of R6/2. Interestingly, the rearing and activity of R6/2 mice were moderately worsened in REGγ nulls at 13 weeks. However, as there was no consistent synergism between R6/2 and REGγ null mice, this is unlikely to reflect a general beneficial role of REGγ in R6/2 phenotype. We therefore conclude that REGγ is not a viable therapeutic target in HD or other polyglutamine diseases.

There are two mechanisms through which mutant polyglutamine tracts have been proposed to impair proteasome function. In the first, although unfolding and degradation of the substrate are initiated, regions that are too tightly aggregated to unfold would be too large to enter the 20S chamber (35). In support of this, it has been shown by FRET and FLIP analysis that proteasomes are in very close association with polyglutamine inclusions and have a slow off-rate, suggesting that polyglutamines become irreversibly associated with proteasomes at inclusion bodies (36). This is consistent with the colocalization of proteasome components with inclusion bodies in brain sections of patients and transgenic mice (9,10,18). Alternatively, the failure of polyglutamine tracts to be degraded by and exit from proteasomes may cause the 26S proteasome to become clogged (20,24,36). Therefore, either the failure of aggregated polyglutamine proteins to enter the proteasome or the proteasome clogging with trapped polyglutamine may inhibit the proteasome from degrading other substrates. However, contrary to these hypotheses, it has been shown in a cell culture system that impairment of the UPS occurs in both the nucleus and the cytoplasm regardless of which compartment the mutant polyglutamine is restricted to (12). This suggests that the impairment of the UPS can be caused by mechanisms other than an aberrant association of polyglutamines with proteasomes.

If irreversible inhibition of proteasomes were a significant factor throughout the R6/2 brain, we would have expected to detect diminished 26S proteasome activity. However, we

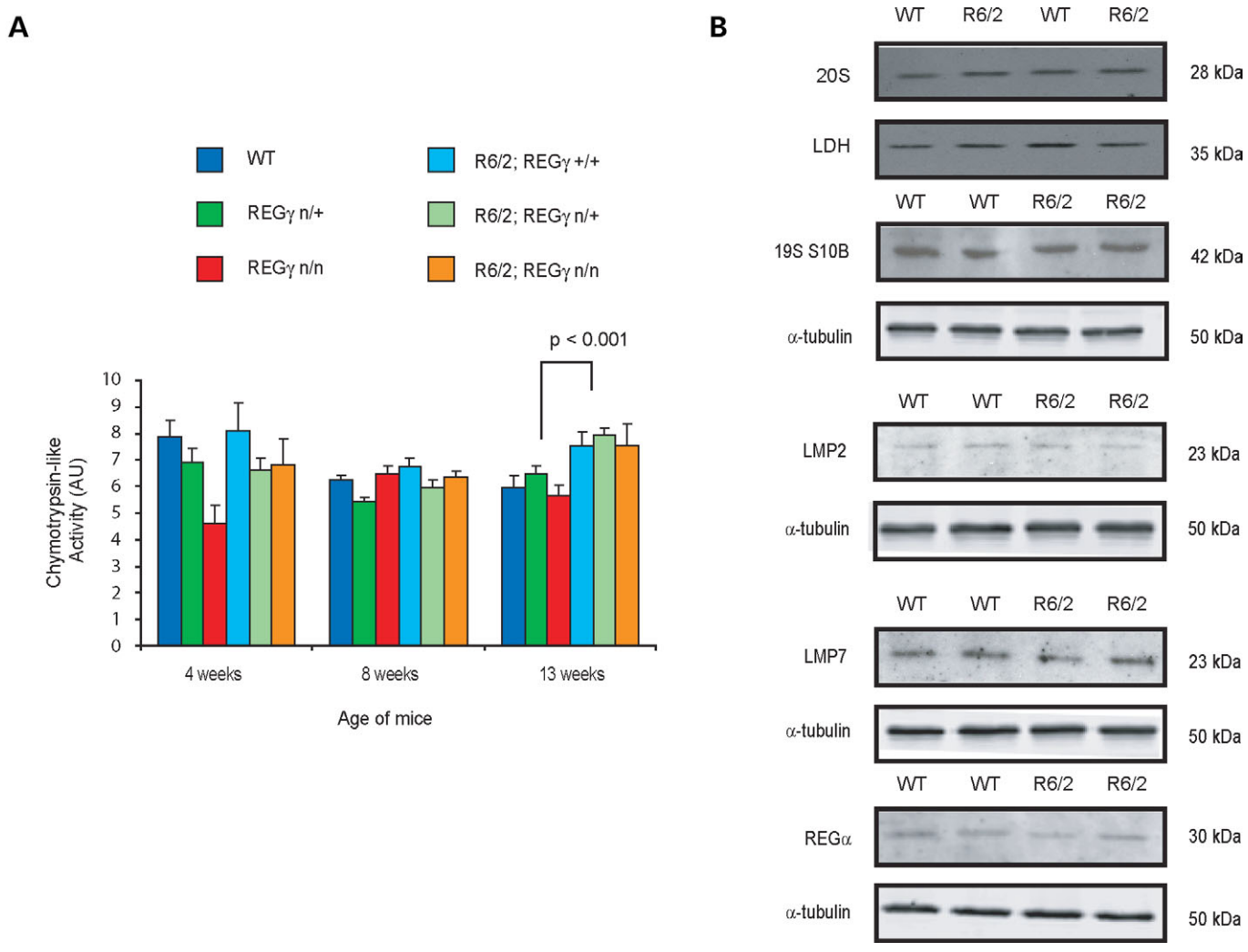

Figure 6. 20S proteasome activity is upregulated in R6/2 mice regardless of REGγ levels. (**A**) Chymotrypsin-like activity of mouse brain extracts is significantly higher in 13-week R6/2 mouse brains when compared with non-R6/2 regardless of REGγ levels. Error bars represent the standard error of the mean. (**B**) Western blot of 12-week R6/2 and WT brain lysates showed no significant difference in levels of 20S proteasome, the 19S S10B subunit, LMP2, LMP7 or REGα. α-tubulin was used as a loading control for all antibodies except the 20S antibody, where LDH was used.

failed to detect lowered 26S activity and even observed a marked increase in the hydrolysis of the proteasome-specific sLLVY fluorogenic peptide. Therefore, although a degree of proteasome clogging/blockage may indeed occur, the degradative capacity of the UPS is not compromised in R6/2 mice. These results are consistent with other studies. For example, no neuronal impairment was detected by a UPS reporter with a UFD signal in SCA7 mice, suggesting that significant proteasome impairment by polyglutamines is not a general occurrence *in vivo* (14).

There is considerable evidence that modulating the UPS alters inclusion body formation (19,37–40), but it is still unknown whether, when and how the UPS contributes to polyglutamine pathogenesis *in vivo*. To date, there is considerable evidence against a UPS impairment in polyglutamine disease mouse models (14–16), and we find no evidence of an impairment in R6/2 mice. In symptomatic HD patients, however, a decrease in proteasome activity was observed at the level of the 20S core (17). Therefore, there is a strong possibility that rather than being a primary cause of toxicity, UPS dysfunction may occur as a consequence of the disease or even by a synergistic effect of polyglutamine stress and the normal human ageing process. Indeed, Seo *et al.* (17) note that they found an increase in 20S activity in the brain of a patient with juvenile HD. This is comparable to the increased proteasome activity in R6/2 and HD94 mice (16). Interestingly, they also find that human HD fibroblasts have lost the ability to upregulate proteasome activity in response to overexpression of the 11S activator REGα. A similar effect has been reported elsewhere whereby neurons expressing mutant polyglutamine fail to increase proteasome activity in response to heat shock, whereas cells expressing WT polyglutamine effectively increase activity in response to heat shock (41). Therefore, it is conceivable that the normal ageing process invokes a level of proteasome activity in healthy neurons which HD neurons cannot reach, resulting in the observed diminution.

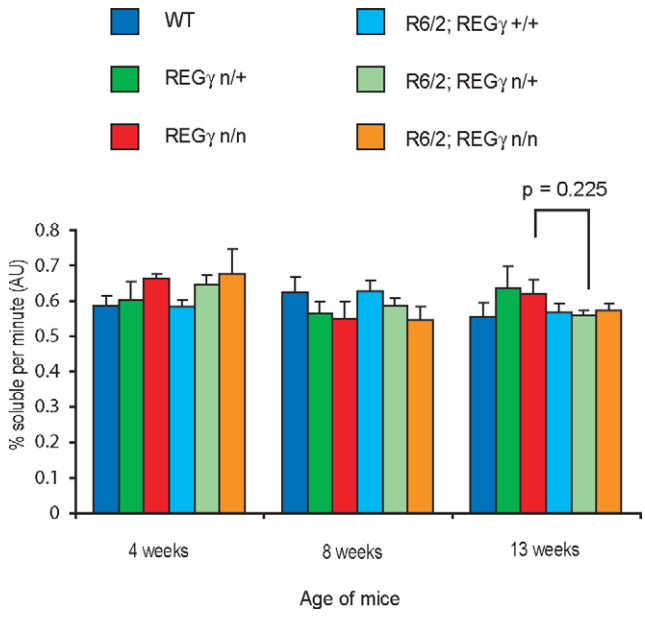

Figure 7. 26S proteasome activity of mouse brain extracts shows no difference between R6/2 and WT brains at any timepoint. There is also no effect of reducing REGγ levels on 26S activity in mouse brains. Error bars represent standard errors of the mean.

In order to try and account for the upregulation of proteasome activity in R6/2 brains, we compared protein levels of various proteasome-associated proteins of 12-week-old R6/2 and WT. We found that 20S proteasome levels were not significantly upregulated in R6/2. However, we did observe that there was in fact a minor but consistent increase in 20S levels in R6/2 at 4, 8 and 13 weeks. Similarly, although LMP7 levels were not significantly upregulated in R6/2, we found that they did tend to be moderately higher from 4 weeks onwards. However, as these modest upregulations do not correlate with the 20S activity increase, their relevance is unclear. We also compared protein levels of the 19S S10B subunit, the immunoproteasome subunit LMP2 and the 11S proteasome activators REGγ and REGα, but found no significant difference between R6/2 and WT. The upregulation of activity in R6/2 mice therefore may be due to an altered association of 20S core with regulators and other subunits, rather than a direct upregulation of proteasomal proteins. For example, it may be the case that although the levels of immunoproteasome subunits LMP2 and LMP7 are unaltered in R6/2, their incorporation into 20S proteasomes may be increased. Similarly, proteasomes may be associated with the REGα/β complex more frequently in R6/2 than in WT, which again could account for increase in activities.

A major issue yet to be resolved is why there appears to be a marked inhibition of the UPS in some cell models of polyglutamine disease (11–13), but strong evidence against an inhibition *in vivo* (14). It could be argued that cell models do not reflect disease pathology as accurately as mouse models. However, an interesting possibility is that different reporter degrons are differentially recognized in disease and WT contexts. In this case, the impairment of the UPS in cell models (11,13) would lie within the ubiquitylation machinery. For example, the specific E2 ubiquitin conjugating enzymes and the E3 ubiquitin ligases that recognize the degrons used in these UPS reporters may be compromised, whereas those that recognize N-end rule and UFD signals used in other studies (8,14) may function to full capacity. In this case, an impairment in the UPS would only affect a subset of proteasome substrates which may or may not appreciably affect the disease process. It will be important to test impairment of the UPS in polyglutamine disease *in vivo* using a mouse expressing a UPS reporter construct similar to that used by Bence *et al.* (11). This will be important to determine definitively whether UPS impairment can be a significant factor in polyglutamine disease.

MATERIALS AND METHODS

Mouse husbandry and genotyping

Mice were housed, and experimental procedures were performed according to the Home Office regulations. Mice had unlimited access to water and number 3 rodent breeding chow (Special Diet Services, Witham, UK) and were subject to a 12 h light (08:00–20:00) and 12 h dark (20:00–08:00) cycles. Mice were housed 5 to a cage with environmental enrichment in the form of paper shred bedding (Enviro-dri, Lillico, Betchworth, UK), a play tunnel (Datesand Ltd, Manchester, UK) and wood shavings (GLP Aspen Chips, Datesand Ltd). The R6/2 mouse colony was maintained by backcrossing R6/2 males to (C57BL/6xCBA) F1 females (B6CBAF1/OlaHsd, Harlan Olac, Bichester, UK). R6/2 mice were identified by polymerase chain reaction (PCR) (29), and the CAG repeat size was determined as described previously (42). REGγ knock-out mice were generated as described previously (25) and maintained on a C57/BL6 background. Mice were identified by PCR of tail-tip DNA in a 25 μl reaction containing 1 μl DNA (100 ng/μl), 3 μl 2 nM dNTPs, 2.5 μl AM buffer [670 mM Tris, 166 mM ammonium sulphate, 20 mM magnesium chloride, 1.7 mg/ml bovine serum albumin (BSA), 0.1 M β-mercaptoethanol], 1 μl forward primer 'a' TCGAGCGAGCACGTACT (100 ng/μl), 1 μl reverse primer CACGATGGACTGGATGGT (100 ng/μl), 1 μl forward primer 'b' CTAACATAACTTACCTTGCC (100 ng/μl), 0.2 μl Promega Taq (5 U/l) and 15.3 μl dH_2O. The reverse primer and forward primer 'a' or forward primer 'b' amplified mutant and WT bands, respectively. Cycling conditions were 95°C 120 s, 30× (95°C 45 s, 50°C 45 s and 72°C 45 s) and 72°C 7 min.

Behavioural analysis

Rotarod and grip strength analysis were performed as described previously (29). Briefly, mice were placed on a modified Ugo Basile 7650 accelerating RotaRod (Linton Instrumentation, UK). At 4 weeks of age, mice were tested on four consecutive days, with three trials per day. At 8, 10 and 12 weeks of age, mice were tested on three consecutive days, with three trials per day. Grip strength was measured as described previously, but using a digital grip strength meter (San Diego Instruments). Mice were weighed weekly to the nearest 0.1 g. Exploratory activity of mice was assessed and statistics performed as recently described (43).

Western blot analysis

Mice were sacrificed by cervical dislocation, and brains were quickly dissected and frozen in isopentane on dry ice. Half brains from REGγ mice were homogenized with a dounce homogenizer in 1 ml sodium phosphate buffer [20 mM sodium phosphate, 1% sodium dodecyl sulphate (SDS), 2 mM phenylmethylsulphonyl fluoride (PMSF) and complete protease inhibitors (Boehringer Mannheim)]. Half brains from R6/2 mice were homogenized in 1% Triton X buffer [1% Triton X-100 in phosphate-buffered saline (PBS) and complete protease inhibitors (Boehringer Mannheim)] for blotting with REGα and REGγ or in sucrose buffer [0.25 M sucrose, 10 mM Tris pH 7 and complete protease inhibitors (Boehringer Mannheim)] for all other antibodies. The protein concentration of the lysates was adjusted to 5 μg/μl using the BCA assay kit (Perbio). Lysates were aliquoted, snap frozen on dry ice and stored at −80°C. Nuclear and cytoplasmic extracts were prepared as described previously (30).

Lysates were thawed on ice before 10–30 μg protein was boiled for 5 min and loaded onto 10% SDS–PAGE gels, separated and blotted onto Protran membranes (Schleicher and Schuell). Membranes were then blocked in 5% non-fat dried milk (NFDM) for 1 h at room temperature and probed with primary antibody in 5% NFDM for 2 h at room temperature or overnight. For chemiluminescent detection, blots were washed three times in Tris-buffered saline (TBS) and probed with horseradish peroxidase (HRP)-linked secondary antibodies in 5% NFDM for 1 h at room temperature. Protein was detected by chemiluminescense (ECL kit, Amersham), according to manufacturer's instructions. For quantification of REGγ and REGα protein levels, blots were probed with Alexa 488/546-attached secondary antibodies and incubated for 1 h at room temperature, then washed three times with TBS in darkness. Protein was detected on a Typhoon 9200 PhosphorImager (Amersham Biosciences), and band intensities were calculated using ImageQuant® software (Molecular® Dynamics). All other protein levels were quantified on a Bio-Rad GS-800 Calibrated Densitometer using Quantity-One® Software. At least four brains of each genotype were used for quantification. Primary antibodies and dilutions were as follows: REGγ (Transduction Laboratories) (mAb, 1:1000), REGα (Affinity Bioreagents) (rabbit pAb, 1:5000), β-actin (AbCam) (mAb, 1:10 000), α-tubulin (Sigma-Aldridge) (mAb, 1:2000), LMP2 (Biomol) (rabbit pAb, 1:2000), LMP7 (Biomol) (rabbit pAb, 1:10 000) and 19S S10B (33) (rabbit pAb, 1:5000). Our lactate dehydrogenase (LDH) antibody was prepared in rabbits using purified porcine lactate dehydrogenase (Calbiochem) as immunogen. Immunoglobulins (IgG) were precipitated from serum with 50% ammonium sulphate, desalted and lyophilized. The resuspended IgG fraction, diluted 1:2000, detects an appropriately sized band of ∼35 kDa. Secondary antibody dilutions were HRP-linked anti-rabbit (Dako) (1:3000) and anti-mouse (Vectastain) (1:5000); Alexa-488 conjugated anti-mouse (Molecular Probes) (1:1000) and Alexa-546 conjugated anti-rabbit (Molecular Probes) (1:1000).

Membranes were stripped by incubation in stripping buffer (100 mM 3-mercaptoethanol, 2% SDS and 62.5 mM Tris–HCl pH 6.7) for 20 min at 50°C with occasional agitation.

Immunohistochemistry and confocal microscopy

Mouse brains were dissected and frozen as described earlier. Sections were cut to a thickness of 15 μm using a cryostat (Bright Instrument Co. Ltd, UK) and fixed in 4% paraformaldehyde for 30 min. Immunohistochemistry for light and confocal microscopy was carried out as described previously (31). Primary antibody dilutions were as follows: REGγ (Biomol) (rabbit pAb, 1:15 000), S830 (sheep pAb, 1:2000) and NeuN (Chemicon) (mAb, 1:500). Biotinylated secondary antibodies from Vector Laboratories were anti-rabbit (1:200) and anti-sheep (1:500) and fluorescent secondary antibodies from Molecular Probes were Alexa-488 anti-mouse (1:400) and Alexa-546 anti-rabbit (1:400). Sections were viewed on a Zeiss light microscope and images were captured using an axiocam, with the help of the Zeiss axiovision software. For colocalization, a Zeiss LSM150 confocal microscope was used.

20S and 26S proteasome assays

Frozen mouse brains were weighed, placed in a 10 ml glass homogenizer and overlaid with 2.5 volumes of lysis buffer (0.25 M sucrose, 10 mM Tris pH 7.0, complete protease inhibitors). Brains were thawed in lysis buffer for 2 min, then homogenized with three passes of a teflon pestle driven by a hand drill. Samples of whole cell extract were then aliquoted into fractions that were either stored at −80°C (26S assays) or kept on ice (20S assays). Protein concentration was determined in duplicate on fresh lysate using Coomassie Plus Protein Assay Reagent (Pierce). Assays were performed in triplicate on three brains of each genotype/timepoint. For each assay, values for 1 min averages were calculated from each reaction (i.e. at 3, 6 and 9 min), and the data pooled for each genotype/timepoint before statistical analysis were carried out (GLM ANOVA).

Assays for 20S proteasome activity were performed using the sLLVY-MCA fluorescent peptide (Peptides International) as a substrate. sLLVY was dissolved at 10 mM in DMSO and diluted to a working stock of 200 μM in reticulocyte buffer (10 mM Tris pH 7.8, 5 mM $MgCl_2$, 10 mM KCl and 1 mM DTT) prior to use. Reaction mixes (100 μl final volume) were prepared in reticulocyte buffer and contained 10 μg of protein, 2.5 μl of an ATP regenerating system (6 mg/ml ATP, 1.2 mg/ml creatine kinase and 60 mg/ml phosphocreatine) and 100 μM of fluorescent peptide substrate. Reactions were incubated at 37°C for 3, 6 and 9 min, quenched with 200 μl of 100% ethanol and read using a Perkin Elmer LS-5 Spectroflourimeter (380 nm excitation/440 nm).

Assays for 26S proteasome activity were performed using iodinated ubiquitin–lysozyme conjugates as substrates. ^{125}I-lysozyme conjugates were prepared according to previously published methods (44) and stored at −80°C. Reaction mixes (100 μl final volume) were prepared in reticulocyte buffer and contained 10 μg of protein, 2.5 μl of an ATP regenerating system and 50 μl of ^{125}I-lysozyme conjugates. Reactions were incubated at 37°C for 3, 6 and 9 min, then quenched by the addition of 800 μl of 1% BSA (dissolved in 10 mM Tris pH 7.0) followed by 100 μl of 100% trichloroacetic acid. Samples were then mixed, incubated on ice for 15 min, centrifuged at 14 000*g* for 15 min and ultimately

analysed on a Beckman Gamma 4000 counter. Both supernatant (800 μl) and pellet were counted. To correct for the amount of supernatant removed, supernatant counts were divided by 0.8, and the corrected supernatant value was ultimately divided by the total counts (soluble plus pellet). All samples were corrected for background soluble counts found in a zero control tube that did not contain brain lysate.

Control assays were performed on normal mouse brain extracts to ensure the accuracy of the proteasome activity measurements. Inhibitor studies demonstrated that both Ub-conjugate (26S) and sLLVY (20S) degradation were proteasome specific. sLLVY was most diagnostic of mouse brain proteasome activity, as the proteasome inhibitors lactacystin and epoxomicin inhibited its degradation by 80–90% (data not shown). Epoxomicin inhibited Ub-conjugate degradation by >80% (data not shown). We attempted to assay the trypsin-like and caspase-like activities of the proteasome using the fluorescent peptides LLR-MCA (Peptides International) and LLE-bNA (Sigma). However, inhibitor controls using epoxomicin and lactacystin indicated that their degradation in mouse brain extracts was not highly proteasome specific. Further control experiments were performed to ensure that enzymatic measurements were in the linear range, where both 20S and 26S enzyme activities were directly proportional to the reaction time and the amount of extract in the reaction mix (data not shown).

Statistics

GLM ANOVA and *post hoc* analysis were performed on Excel and Minitab for behavioural and proteasome activity assays. For western blot quantification, Student's *t*-test was performed.

ACKNOWLEDGEMENTS

The authors wish to thank Emma Hockly, Jamie Tse and Amy Barker for help with behavioural testing and analysis. This work was supported by a Wellcome Trust Prize studentship to J.S.B. (73061) and grants from the Wellcome Trust (060360 and 066270), Huntington's Disease Society of America Coalition for the Cure, Hereditary Disease Foundation and NIH (5R01NS0 42892-02). Funding to pay the Open Access publication charges for this article was provided by the Wellcome Trust.

Conflict of Interest statement. None declared.

REFERENCES

1. Davies, S.W., Turmaine, M., Cozens, B.A., DiFiglia, M., Sharp, A.H., Ross, C.A., Scherzinger, E., Wanker, E.E., Mangiarini, L. and Bates, G.P. (1997) Formation of neuronal intranuclear inclusions underlies the neurological dysfunction in mice transgenic for the HD mutation. *Cell*, **90**, 537–548.
2. DiFiglia, M., Sapp, E., Chase, K.O., Davies, S.W., Bates, G.P., Vonsattel, J.P. and Aronin, N. (1997) Aggregation of huntingtin in neuronal intranuclear inclusions and dystrophic neurites in brain. *Science*, **277**, 1990–1993.
3. Scherzinger, E., Lurz, R., Turmaine, M., Mangiarini, L., Hollenbach, B., Hasenbank, R., Bates, G.P., Davies, S.W., Lehrach, H. and Wanker, E.E. (1997) Huntingtin-encoded polyglutamine expansions form amyloid-like protein aggregates *in vitro* and *in vivo*. *Cell*, **90**, 549–558.
4. Yang, W., Dunlap, J.R., Andrews, R.B. and Wetzel, R. (2002) Aggregated polyglutamine peptides delivered to nuclei are toxic to mammalian cells. *Hum. Mol. Genet.*, **11**, 2905–2917.
5. Arrasate, M., Mitra, S., Schweitzer, E.S., Segal, M.R. and Finkbeiner, S. (2004) Inclusion body formation reduces levels of mutant huntingtin and the risk of neuronal death. *Nature*, **431**, 805–810.
6. Saudou, F., Finkbeiner, S., Devys, D. and Greenberg, M.E. (1998) Huntingtin acts in the nucleus to induce apoptosis but death does not correlate with the formation of intranuclear inclusions. *Cell*, **95**, 55–66.
7. Schaffar, G., Breuer, P., Boteva, R., Behrends, C., Tzvetkov, N., Strippel, N., Sakahira, H., Siegers, K., Hayer-Hartl, M. and Hartl, F.U. (2004) Cellular toxicity of polyglutamine expansion proteins: mechanism of transcription factor deactivation. *Mol. Cell*, **15**, 95–105.
8. Verhoef, L.G., Lindsten, K., Masucci, M.G. and Dantuma, N.P. (2002) Aggregate formation inhibits proteasomal degradation of polyglutamine proteins. *Hum. Mol. Genet.*, **11**, 2689–2700.
9. Cummings, C.J., Mancini, M.A., Antalffy, B., DeFranco, D.B., Orr, H.T. and Zoghbi, H.Y. (1998) Chaperone suppression of aggregation and altered subcellular proteasome localization imply protein misfolding in SCA1. *Nat. Genet.*, **19**, 148–154.
10. Schmidt, T., Lindenberg, K.S., Krebs, A., Schols, L., Laccone, F., Herms, J., Rechsteiner, M., Riess, O. and Landwehrmeyer, G.B. (2002) Protein surveillance machinery in brains with spinocerebellar ataxia type 3: redistribution and differential recruitment of 26S proteasome subunits and chaperones to neuronal intranuclear inclusions. *Ann. Neurol.*, **51**, 302–310.
11. Bence, N.F., Sampat, R.M. and Kopito, R.R. (2001) Impairment of the ubiquitin–proteasome system by protein aggregation. *Science*, **292**, 1552–1555.
12. Bennett, E.J., Bence, N.F., Jayakumar, R. and Kopito, R.R. (2005) Global impairment of the ubiquitin–proteasome system by nuclear or cytoplasmic protein aggregates precedes inclusion body formation. *Mol. Cell*, **17**, 351–365.
13. Park, Y., Hong, S., Kim, S.J. and Kang, S. (2005) Proteasome function is inhibited by polyglutamine-expanded ataxin-1, the SCA1 gene product. *Mol. Cells*, **19**, 23–30.
14. Bowman, A.B., Yoo, S.Y., Dantuma, N.P. and Zoghbi, H.Y. (2005) Neuronal dysfunction in a polyglutamine disease model occurs in the absence of ubiquitin–proteasome system impairment and inversely correlates with the degree of nuclear inclusion formation. *Hum. Mol. Genet.*, **14**, 679–691.
15. Zhou, H., Cao, F., Wang, Z., Yu, Z.X., Nguyen, H.P., Evans, J., Li, S.H. and Li, X.J. (2003) Huntingtin forms toxic NH2-terminal fragment complexes that are promoted by the age-dependent decrease in proteasome activity. *J. Cell. Biol.*, **163**, 109–118.
16. Diaz-Hernandez, M., Hernandez, F., Martin-Aparicio, E., Gomez-Ramos, P., Moran, M.A., Castano, J.G., Ferrer, I., Avila, J. and Lucas, J.J. (2003) Neuronal induction of the immunoproteasome in Huntington's disease. *J. Neurosci.*, **23**, 11653–11661.
17. Seo, H., Sonntag, K.C. and Isacson, O. (2004) Generalized brain and skin proteasome inhibition in Huntington's disease. *Ann. Neurol.*, **56**, 319–328.
18. Jana, N.R., Zemskov, E.A., Wang, G. and Nukina, N. (2001) Altered proteasomal function due to the expression of polyglutamine-expanded truncated N-terminal huntingtin induces apoptosis by caspase activation through mitochondrial cytochrome *c* release. *Hum. Mol. Genet.*, **10**, 1049–1059.
19. Cummings, C.J., Reinstein, E., Sun, Y., Antalffy, B., Jiang, Y., Ciechanover, A., Orr, H.T., Beaudet, A.L. and Zoghbi, H.Y. (1999) Mutation of the E6-AP ubiquitin ligase reduces nuclear inclusion frequency while accelerating polyglutamine-induced pathology in SCA1 mice. *Neuron*, **24**, 879–892.
20. Venkatraman, P., Wetzel, R., Tanaka, M., Nukina, N. and Goldberg, A.L. (2004) Eukaryotic proteasomes cannot digest polyglutamine sequences and release them during degradation of polyglutamine-containing proteins. *Mol. Cell*, **14**, 95–104.
21. Michalik, A. and Van Broeckhoven, C. (2004) Proteasome degrades soluble expanded polyglutamine completely and efficiently. *Neurobiol. Dis.*, **16**, 202–211.
22. Kaytor, M.D., Wilkinson, K.D. and Warren, S.T. (2004) Modulating huntingtin half-life alters polyglutamine-dependent aggregate formation and cell toxicity. *J. Neurochem.*, **89**, 962–973.
23. Li, J. and Rechsteiner, M. (2001) Molecular dissection of the 11S REG (PA28) proteasome activators. *Biochimie*, **83**, 373–383.

24. Goellner, G.M. and Rechsteiner, M. (2003) Are Huntington's and polyglutamine-based ataxias proteasome storage diseases? *Int. J. Biochem. Cell Biol.*, **35**, 562–571.
25. Murata, S., Kawahara, H., Tohma, S., Yamamoto, K., Kasahara, M., Nabeshima, Y., Tanaka, K. and Chiba, T. (1999) Growth retardation in mice lacking the proteasome activator PA28gamma. *J. Biol. Chem.*, **274**, 38211–38215.
26. Wojcik, C., Tanaka, K., Paweletz, N., Naab, U. and Wilk, S. (1998) Proteasome activator (PA28) subunits, alpha, beta and gamma (Ki antigen) in NT2 neuronal precursor cells and HeLa S3 cells. *Eur. J. Cell. Biol.*, **77**, 151–160.
27. Masson, P., Lundgren, J. and Young, P. (2003) *Drosophila* proteasome regulator REGgamma: transcriptional activation by DNA replication-related factor DREF and evidence for a role in cell cycle progression. *J. Mol. Biol.*, **327**, 1001–1012.
28. Carter, R.J., Lione, L.A., Humby, T., Mangiarini, L., Mahal, A., Bates, G.P., Dunnett, S.B. and Morton, A.J. (1999) Characterization of progressive motor deficits in mice transgenic for the human Huntington's disease mutation. *J. Neurosci.*, **19**, 3248–3257.
29. Hockly, E., Woodman, B., Mahal, A., Lewis, C.M. and Bates, G. (2003) Standardization and statistical approaches to therapeutic trials in the R6/2 mouse. *Brain Res. Bull.*, **61**, 469–479.
30. Hay, D.G., Sathasivam, K., Tobaben, S., Stahl, B., Marber, M., Mestril, R., Mahal, A., Smith, D.L., Woodman, B. and Bates, G.P. (2004) Progressive decrease in chaperone protein levels in a mouse model of Huntington's disease and induction of stress proteins as a therapeutic approach. *Hum. Mol. Genet.*, **13**, 1389–1405.
31. Smith, D.L., Portier, R., Woodman, B., Hockly, E., Mahal, A., Klunk, W.E., Li, X.J., Wanker, E., Murray, K.D. and Bates, G.P. (2001) Inhibition of polyglutamine aggregation in R6/2 HD brain slices-complex dose–response profiles. *Neurobiol. Dis.*, **8**, 1017–1026.
32. Hoffman, L., Pratt, G. and Rechsteiner, M. (1992) Multiple forms of the 20 S multicatalytic and the 26 S ubiquitin/ATP-dependent proteases from rabbit reticulocyte lysate. *J. Biol. Chem.*, **267**, 22362–22368.
33. Gorbea, C., Taillandier, D. and Rechsteiner, M. (2000) Mapping subunit contacts in the regulatory complex of the 26 S proteasome. S2 and S5b form a tetramer with ATPase subunits S4 and S7. *J. Biol. Chem.*, **275**, 875–882.
34. Rechsteiner, M. and Hill, C.P. (2005) Mobilizing the proteolytic machine: cell biological roles of proteasome activators and inhibitors. *Trends Cell Biol.*, **15**, 27–33.
35. Navon, A. and Goldberg, A.L. (2001) Proteins are unfolded on the surface of the ATPase ring before transport into the proteasome. *Mol. Cell*, **8**, 1339–1349.
36. Holmberg, C.I., Staniszewski, K.E., Mensah, K.N., Matouschek, A. and Morimoto, R.I. (2004) Inefficient degradation of truncated polyglutamine proteins by the proteasome. *EMBO J.*, **23**, 4307–4318.
37. Peters, P.J., Ning, K., Palacios, F., Boshans, R.L., Kazantsev, A., Thompson, L.M., Woodman, B., Bates, G.P. and D'Souza-Schorey, C. (2002) Arfaptin 2 regulates the aggregation of mutant huntingtin protein. *Nat. Cell Biol.*, **4**, 240–245.
38. Nollen, E.A., Garcia, S.M., van Haaften, G., Kim, S., Chavez, A., Morimoto, R.I. and Plasterk, R.H. (2004) Genome-wide RNA interference screen identifies previously undescribed regulators of polyglutamine aggregation. *Proc. Natl Acad. Sci. USA*, **101**, 6403–6408.
39. Warrick, J.M., Morabito, L.M., Bilen, J., Gordesky-Gold, B., Faust, L.Z., Paulson, H.L. and Bonini, N.M. (2005) Ataxin-3 suppresses polyglutamine neurodegeneration in *Drosophila* by a ubiquitin-associated mechanism. *Mol. Cell*, **18**, 37–48.
40. Jana, N.R., Dikshit, P., Goswami, A., Kotliarova, S., Murata, S., Tanaka, K. and Nukina, N. (2005) Co-chaperone CHIP associates with expanded polyglutamine protein and promotes their degradation by proteasomes. *J. Biol. Chem.*, **280**, 11635–11640.
41. Ding, Q., Lewis, J.J., Strum, K.M., Dimayuga, E., Bruce-Keller, A.J., Dunn, J.C. and Keller, J.N. (2002) Polyglutamine expansion, protein aggregation, proteasome activity, and neural survival. *J. Biol. Chem.*, **277**, 13935–13942.
42. Mangiarini, L., Sathasivam, K., Seller, M., Cozens, B., Harper, A., Hetherington, C., Lawton, M., Trottier, Y., Lehrach, H., Davies, S.W. *et al.* (1996) Exon 1 of the HD gene with an expanded CAG repeat is sufficient to cause a progressive neurological phenotype in transgenic mice. *Cell*, **87**, 493–506.
43. Hockly, E., Tse, J., Barker, A.L., Moolman, D.L., Beunard, J.L., Revington, A.P., Holt, K., Sunshine, S., Moffitt, H., Sathasivam, K. *et al.* (2005) Evaluation of the benzothiazole aggregation inhibitors riluzole and PGL-135 as therapeutics for Huntington's disease. *Neurobiol. Dis.*, in press.
44. Hough, R. and Rechsteiner, M. (1986) Ubiquitin–lysozyme conjugates. Purification and susceptibility to proteolysis. *J. Biol. Chem.*, **261**, 2391–2399.